AD-A073 416 WEAPONS SYSTEMS RESEARCH LAB ADELAIDE (AUSTRALIA) F/G 20/4
AN ATTEMPTED EXTENSION OF A FINITE ELEMENT SOLUTION TO AXISYMME--ETC(U)
NOV 78 M K HASELGROVE

UNCLASSIFIED WSRL-0056-TR NL

| OF |
AD A073416

END
DATE FILMED
10-79
DDC

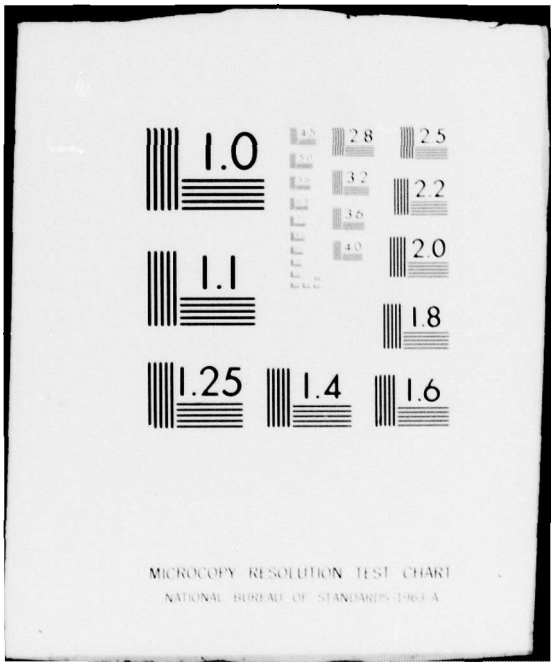
1.0
1.1
1.25
1.4
1.6
2.8
3.2
3.6
4.0
2.5
2.2
2.0
1.8
MICROCOPY RESOLUTION TEST CHART
NATIONAL BUREAU OF STANDARDS 1963-A

(12) LEVEL II

WSRL-0056-TR

AR-001-422

AD A073416

DEPARTMENT OF DEFENCE

DEFENCE SCIENCE AND TECHNOLOGY ORGANISATION

WEAPONS SYSTEMS RESEARCH LABORATORY

DEFENCE RESEARCH CENTRE SALISBURY
SOUTH AUSTRALIA

TECHNICAL REPORT

WSRL-0056-TR

AN ATTEMPTED EXTENSION OF A FINITE ELEMENT SOLUTION TO AXISYMMETRIC POTENTIAL FLOW

M.K. HASELGROVE

Approved for Public Release

NOVEMBER 1978

COPY No. 36

DEPARTMENT OF DEFENCE

DEFENCE SCIENCE AND TECHNOLOGY ORGANISATION

WEAPONS SYSTEMS RESEARCH LABORATORY

AR-001-422

(9) TECHNICAL REPORT,

(14) WSRL-0056-TR

(6) AN ATTEMPTED EXTENSION OF A FINITE ELEMENT SOLUTION TO AXISYMMETRIC POTENTIAL FLOW

(10) M.K. Haselgrove

(11) Nov 78

(12) 25 p.

SUMMARY

A Galerkin finite element method, which has been successfully applied to two-dimensional inviscid flow, has been applied to axisymmetric potential flow. Solutions have been sought for three alternative formulations using different representations for the velocity components. Two of the formulations produced only poor results, while the third gave no worthwhile results at all. Possible reasons for the failure of the method are discussed.

Approved for Public Release

POSTAL ADDRESS: Chief Superintendent, Weapons Systems Research Laboratory, Box 2151, G.P.O., Adelaide, South Australia, 5001.

DOCUMENT CONTROL DATA SHEET

Security classification of this page: UNCLASSIFIED

1 DOCUMENT NUMBERS	
AR Number:	AR-001-422
Report Number:	WSRL-0056-TR
Other Numbers:	

2 SECURITY CLASSIFICATION	
a. Complete Document:	UNCLASSIFIED
b. Title in Isolation:	UNCLASSIFIED
c. Summary in Isolation:	UNCLASSIFIED

3 TITLE

AN ATTEMPTED EXTENSION OF A FINITE ELEMENT SOLUTION TO AXISYMMETRIC POTENTIAL FLOW

4 PERSONAL AUTHOR(S):

M.K. Haselgrove

5 DOCUMENT DATE: November 1978

6 6.1 TOTAL NUMBER OF PAGES: 24

6.2 NUMBER OF REFERENCES: 6

7 7.1 CORPORATE AUTHOR(S):

Weapons Systems Research Laboratory

7.2 DOCUMENT SERIES AND NUMBER

Weapons Systems Research Laboratory 0056-TR

8 REFERENCE NUMBERS	
a. Task:	
b. Sponsoring Agency:	

9 COST CODE: 331202

10 IMPRINT (Publishing organisation)

Defence Research Centre Salisbury

11 COMPUTER PROGRAM(S) (Title(s) and language(s))

12 RELEASE LIMITATIONS (of the document):

Approved for Public Release.

12.0	OVERSEAS	NO		P.R.	1	A		B		C		D		E	

Security classification of this page: UNCLASSIFIED

Security classification of this page: UNCLASSIFIED

13 ANNOUNCEMENT LIMITATIONS (of the information on these pages):

No limitation.

14 DESCRIPTORS:

a. EJC Thesaurus Terms

Axisymmetric bodies
Incompressible flow
Inviscid flow
Axisymmetric flow
Fluid flow
Fluid dynamics
Computation
Boundary layer flow

b. Non-Thesaurus Terms

Galerkin finite element
Finite element method
Weighted residual method

15 COSATI CODES:

2004

16 LIBRARY LOCATION CODES (for libraries listed in the distribution):

17 SUMMARY OR ABSTRACT:
(if this is security classified, the announcement of this report will be similarly classified)

A Galerkin finite element method, which has been successfully applied to two-dimensional inviscid flow, has been applied to axisymmetric potential flow. Solutions have been sought for three alternative formulations using different representations for the velocity components. Two of the formulations produced only poor results, while the third gave no worthwhile results at all. Possible reasons for the failure of the method are discussed.

Security classification of this page: UNCLASSIFIED

TABLE OF CONTENTS

LIST OF FIGURES

1. INTRODUCTION

The finite element method has been used successfully in recent times to solve various fluid-flow problems. The apparent generality of the method, and its ease of handling arbitrary flow boundaries, led to its adoption as a basis for work in computational aerodynamics. The long-term aim of the work is to replace some elements of wind-tunnel testing of missile aerodynamics with computer simulation techniques and thereby gain from the configurational flexibility and time saving of computational methods. However, reduced staff ceilings have necessitated the redeployment of resources on work with more immediate benefits and, as a consequence, the finite element work is being terminated by this report.

The project was initiated by Fletcher, who in reference 1 successfully applied the method to two-dimensional, incompressible inviscid flow, and later in reference 2 extended the flow regime to include the subsonic case. The present work was intended as an extension of Fletcher's two-dimensional results to axisymmetric geometries, starting with the inviscid, incompressible case. The formulation of the problem follows that recommended in reference 1, and the program used for solution has subroutines copied or adapted from those used for the results in reference 1.

It should be noted that standard programs are available which use singularity distributions to solve the present problem, for example the method of Albone (ref.3) which uses minimal CPU time but is limited to 'smooth' profiles, and the much more general method of Hess and Smith(ref.4). From the results of reference 1 it is doubtful whether a finite element solution to the present problem would be much more efficient in terms of computing time than others already in use. The benefit of the present work therefore, is dependent on its future extension to more complicated flow regimes, such as in reference 2, where the singularity methods cannot be applied.

2. APPLICATION OF F.E.M. TO AXISYMMETRIC POTENTIAL FLOW

2.1 Field equations

The governing equations for the present problem, in terms of the radial and longitudinal velocity components u and v (see figure 1), are the continuity equation

$$\frac{1}{r}\frac{\partial}{\partial r}(ru) + \frac{\partial v}{\partial z} = 0 \qquad (1)$$

and the equation of conservation of vorticity

$$\frac{\partial u}{\partial z} - \frac{\partial v}{\partial r} = 0, \qquad (2)$$

where r and z are radial and longitudinal coordinates as shown in figure 1.

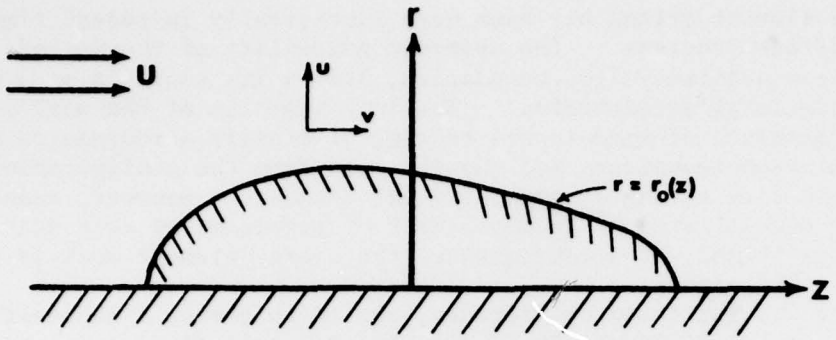

Figure 1. Coordinate system

To complete the problem the boundary conditions are: that the velocity must assume the free-stream value U in the far-field, and that the axis of symmetry and body surface must form a streamline of the flow. That is,

$$\begin{aligned} &u \to 0, \\ &v \to U, \quad \text{as } R = (r^2 + z^2)^{\frac{1}{2}} \to \infty, \\ &u = 0 \quad \text{on} \quad r = 0, \end{aligned} \tag{3}$$

and $u = v.\ r_0'(z)$ on the body surface $r = r_0(z)$.

Equations (1) to (3) are identical to those solved in reference 1 except for the non-linear term in (1). This term requires a modified formulation from that used in reference 1.

2.2 Finite element representation

Following the conclusions of Fletcher(ref.1) a Galerkin formulation with quadratic rectangular elements of 'Serendipity' type was chosen. This formulation is a Method of Weighted Residuals, where the weighting function at each grid point is the shape function at that point. These shape functions, which are given in Appendix I, are chosen so that the isoparametric transformation

$$x = \sum_{i=1}^{8} N_i(\xi,\eta)\, x_i \qquad \text{where } x = r \text{ or } z, \tag{4}$$

transforms axisymmetric elements with nodes (r_i, z_i) in the (r,z) plane into square elements with nodes (ξ_i, η_i) in the (ξ,η) plane, where $\xi_i = \pm 1$ and $\eta_i = \pm 1$. The transformation relates the shape functions in the two planes as

$$N_i(\xi,\eta) = M_i(r,z), \tag{5}$$

where the point (ξ,η) transforms into (r,z) under (4).

Full details of this finite element representation and the associated shape functions $N_i(\xi,\eta)$ can be found in reference 1. Its application to the present problem can proceed in several ways, as follows.

2.2.1 Definition of new flow variable

Multiplying (1) and (2) by r and defining the new flow variable

$$\mu = ru \tag{6}$$

gives

$$\frac{\partial \mu}{\partial r} + r\frac{\partial v}{\partial z} = 0 \tag{7}$$

and

$$\frac{\partial \mu}{\partial z} - r\frac{\partial v}{\partial r} = 0. \tag{8}$$

With the representation in terms of the nodal values,

$$y = \sum_i M_i(r,z)y_i \qquad \text{where } y = \mu \text{ or } v, \tag{9}$$

and where $\sum_i$ means the sum over all contributing nodes i,

the residuals of (7) and (8) are given by

$$R_1 = \sum_i \frac{\partial M_i}{\partial r}\mu_i + r\sum_i \frac{\partial M_i}{\partial z} v_i \tag{10}$$

and

$$R_2 = \sum_i \frac{\partial M_i}{\partial z}\mu_i - r\sum_i \frac{\partial M_i}{\partial r} v_i. \tag{11}$$

The Galerkin formulation

$$\iint_S M_j R_i \, dr\,dz = 0 \qquad \text{for } i = 1,2 \tag{12}$$

where S is the region of the (r,z) plane occupied by the flow field, then gives two algebraic equations at each node point j:

$$\sum_i (a_{ji}\mu_i + b_{ji}v_i) = 0 \tag{13}$$

and

$$\sum_i (c_{ji}\mu_i - d_{ji}\nu_i) = 0, \tag{14}$$

where

$$\begin{aligned} a_{ji} &= \iint_S M_j \frac{\partial M_i}{\partial r}\, dr\, dz, \\ b_{ji} &= \int_S M_j r \frac{\partial M_i}{\partial z}\, dr\, dz, \\ c_{ji} &= \iint_S M_j \frac{\partial M_i}{\partial z}\, dr\, dz \end{aligned} \tag{15}$$

and

$$d_{ji} = \iint_S M_j r \frac{\partial M_i}{\partial r}\, dr\, dz.$$

Because the shape functions $M_k(r,z)$ are defined to be zero in elements not including the k^{th} node, the integrals in (15) are actually evaluated only over the elements common to the j^{th} and i^{th} nodes. This is indicated hereafter by deleting the subscript S from the integral sign.

By transforming the integrals to the iso-parametric plane as described in reference 1 and applying (4) it can readily be shown that

$$\begin{aligned} a_{ji} &= \sum_k G_{jik} z_k, \\ b_{ji} &= \sum_{k,l} D_{jikl} r_k r_l, \\ c_{ji} &= \sum_k G_{jik} r_k \end{aligned} \tag{16}$$

and

$$d_{ji} = -\sum_{k,l} D_{jikl} z_k r_l,$$

where

$$G_{jik} = \iint N_j \left[\frac{\partial N_i}{\partial \xi} \frac{\partial N_k}{\partial \eta} - \frac{\partial N_i}{\partial \eta} \frac{\partial N_k}{\partial \xi} \right] d\xi\, d\eta \tag{17}$$

and

$$D_{jikl} = \iint N_l N_j \left[\frac{\partial N_i}{\partial \xi} \frac{\partial N_k}{\partial \eta} - \frac{\partial N_i}{\partial \eta} \frac{\partial N_k}{\partial \xi} \right] d\xi\, d\eta.$$

2.2.2 Explicit (u,v) formulation

The representation

$$y = \sum_i M_i(r,z)y_i \qquad \text{with } y = u \text{ or } v \tag{18}$$

can be used to express (2) in a form identical to that given for the two dimensional vorticity equation in reference 1 and this, together with the substitution

$$\mu_i = r_i v_i \tag{19}$$

in (13), gives (1) and (2) in terms of the unknown nodal velocity components u_i, v_i, as

$$\sum_i (a_{ji} r_i u_i + b_{ji} v_i) = 0 \tag{20}$$

and

$$\sum_i (c_{ji} u_i - a_{ji} v_i) = 0, \tag{21}$$

where a_{ji}, b_{ji} and c_{ji} are as defined in (15) and (16). Note that this formulation is somewhat inconsistent, in that (21) assumes the representation (18) while (20) assumes (9). This choice is determined by the necessity to make the resulting integrals amenable to the iso-parametric transformation.

An alternative formulation which may be more consistent in this respect is derived by substituting

$$\mu = (\sum_k M_k r_k).(\sum_i M_i u_i) \tag{22}$$

into (7) which gives

$$\sum_i (\sum_k a_{jik} r_k u_i + b_{ji} v_i) = 0, \tag{23}$$

where

$$\begin{aligned} a_{jik} &= \iint M_j \frac{\partial}{\partial r}(M_k M_i)\, dr\, dz \\ &= \sum_1 \iint N_j \left\{ N_k \left[\frac{\partial N_i}{\partial \xi} \frac{\partial N_1}{\partial \eta} - \frac{\partial N_i}{\partial \eta} \frac{\partial N_1}{\partial \xi} \right] \right. \\ &\qquad \left. + N_i \left[\frac{\partial N_k}{\partial \xi} \frac{\partial N_1}{\partial \eta} - \frac{\partial N_k}{\partial \eta} \frac{\partial N_1}{\partial \xi} \right] \right\} d\xi\, d\eta . z_1 \end{aligned} \tag{24}$$

$$= \sum_{1}' (D_{jilk} + D_{jkli})\, z_1$$

with D_{jilk} defined in (17). The other equation, (21), remains unchanged.

2.3 Boundary conditions

The far-field limit of the flow field is taken as the semi-circle $R = (r^2 + z^2)^{\frac{1}{2}} = R_0$, and all velocities are scaled with respect to the free-stream velocity U. Hence for the explicit formulations described in 2.2.2 above, if the i^{th} node is on the boundary the conditions (3) become

$$\left.\begin{aligned} u_i &= 0 \\ v_i &= 1 \end{aligned}\right\} \text{ on } R = R_0,$$

$$u_i = 0 \quad \text{on the axis of symmetry } r = 0, \tag{25}$$

$$\text{and} \quad u_i = v_i r_0'(z_i) \text{ on the body surface.}$$

For the (μ, v) formulation (Section 2.2.1) an additional condition may be required on the axis of symmetry, since the condition $\mu_i = 0$ does not imply that $u_i = 0$. Consider an element on the axis as shown in figure 2 with the corresponding iso-parametric element.

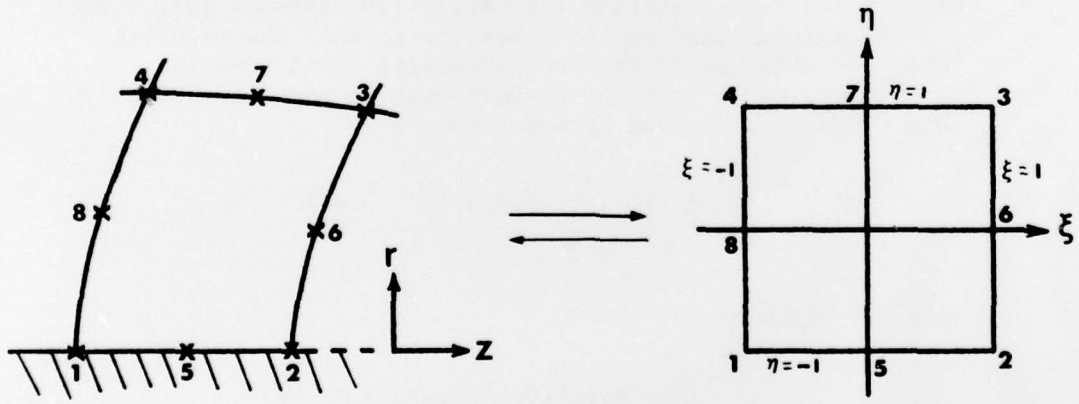

Figure 2. Iso-parametric transformation for axial element

Using the shape functions given in Appendix 1 together with (4) and (9), we can write down the finite-element representation of μ and r on the 3,6,2 boundary of the element (i.e. the $\xi = 1$ boundary of the iso-parametric element) as

$$\mu_s = r_s u_s = \tfrac{1}{2}\eta(1 + \eta)\,\mu_3 + (1 - \eta^2)\,\mu_6 \tag{26}$$

and

$$r_s = \tfrac{1}{2}\eta(1+\eta)r_3 + (1-\eta^2)r_6 . \tag{27}$$

Hence

$$u_s(\eta) = \frac{\mu_s}{r_s} = \frac{\tfrac{1}{2}\eta\,\mu_3 + (1-\eta)\mu_6}{\tfrac{1}{2}\eta\,r_3 + (1-\eta)r_6} . \tag{28}$$

The axis condition $u_s(-1) = 0$ then gives

$$\mu_6 = \tfrac{1}{4}\mu_3 \tag{29}$$

provided $r_6 \neq r_{3/4}$.

Similarly the value on the median line 7,5 ($\xi = 0$ in the iso-parametric element) can be written as

$$x_m(\eta) = \tfrac{1}{4}(\eta^2-1)(x_3+x_4) + \tfrac{1}{2}(1-\eta^2)(x_6+x_8) + \tfrac{1}{2}(1+\eta)x_7 \tag{30}$$

where $x = \mu$ or r. Thus the radial velocity component is given by

$$u_m(\eta) = \frac{\mu_m}{r_m} = \frac{\tfrac{1}{4}(\eta-1)(\mu_3+\mu_4) + \tfrac{1}{2}(1-\eta)(\mu_6+\mu_8) + \tfrac{1}{2}\mu_7}{\tfrac{1}{4}(\eta-1)(r_3+r_4) + \tfrac{1}{2}(1-\eta)(r_6+r_8) + \tfrac{1}{2}r_7} \tag{31}$$

and the axis condition $u_m(-1) = 0$, together with (29) applied at nodes 1 and 2, then gives

$$\mu_7 = (\mu_3 + \mu_4)/2. \tag{32}$$

By applying (29) and (32) the number of unknown nodal μ values in each axial element is reduced from five to two. The actual representation for μ in the iso-parametric element can be shown by substitution to be

$$\mu(\xi,\eta) = \frac{(1+\eta)^2}{8}\left[\mu_3(1+\xi) + \mu_4(1-\xi)\right] , \tag{33}$$

that is, linear in ξ but still quadratic in η. In the (r,z) plane it can be deduced from (1) and (2) that $u = O(r)$ near $r = 0$, which implies a form such as

$$\mu = r^2 f(z) \tag{34}$$

in the axial elements. If we choose

$$\begin{aligned} r_6 &= r_3/2, \\ r_8 &= r_4/2, \\ r_7 &= (r_3 + r_4)/2, \end{aligned} \tag{35}$$

then the iso-parametric transformation for r becomes linear, that is

$$r = \frac{1+\eta}{4}\left[r_3(1+\xi) + r_4(1-\xi) \right]. \tag{36}$$

Thus we can see from (33), (34) and (36) that μ has the required form in the (r,z) plane if the geometrical conditions (35) are satisfied and in addition,

$$z = z(\xi) \tag{37}$$

This last condition can be shown to be true only if

$$\begin{aligned} & z_1 = z_8 = z_4 , \\ & z_5 = z_7 , \\ \text{and} \quad & z_2 = z_6 = z_3 . \end{aligned} \tag{38}$$

Thus we deduce that, for the (μ,v) formulation, the elements adjacent to the axis of symmetry should be constructed to satisfy (35) and (38). Since the choice of the finite-element grid is largely arbitrary, satisfying these geometrical constraints presents no problems except for those elements containing the front or rear stagnation points, in which three nodes lie on the body surface and (38) cannot generally be satisfied. The boundary conditions for the (μ,v) formulation are then

$$\begin{aligned} &\left.\begin{aligned} \mu_i &= 0 \\ v_i &= 1 \end{aligned}\right\} \text{on } R = R_0 , \\ &\mu_i = 0 \quad \text{on } r = 0 , \\ &\mu_i = v_i r_0'(z_i) r_0(z_i) \text{ on } r = r_0(z) , \end{aligned} \tag{39}$$

together with (29) and (32).

At those nodes where one or both of the velocity components are known, only one or none of the Galerkin equations was applied, to equalise the total numbers of equations and unknowns. For the (μ,v) formulation either (29) or (32) replaced one of the Galerkin equations at the appropriate side node in the axial elements.

The far-field condition on v gives rise to a non-zero right-hand side in the matrix form of the equations of motion. This can then be solved for the nodal unknowns, in the present case by using the same sparse-matrix inversion routine as described in reference 1.

2.4 Order of the numerical integration

As in reference 1, two-dimensional Gaussian quadrature was chosen to evaluate expressions such as (17) because an m^{th} order quadrature can integrate exactly, in an analytical sense, polynomial integrands of order (2m-1) or less. The polynomial order is dependent on the order of the composite shape functions which in this case is two or one (see Appendix 1). However the total order can be reduced by the differencing factor in the integrand. Thus for example, the maximum polynomial order of the integrands in (17) is expected to be five and seven respectively, but could be as low as two and three.

Fletcher(ref.5) has found that improved accuracy may result from reducing the order of integration by one from that required to give an exact result. The effect of this 'reduced' integration was briefly examined in the present work, although it should be realised that such integration is still exact for many of the lower-order integrals. It is clear that complete reduced integration would require a variable-order integration routine and would nullify many of the advantages of the iso-parametric formulation, and for this reason was not attempted in the present work.

2.5 Geometry of the flow field

The body half-profile chosen was an ellipse of unit half-thickness and length 2, to which was added a sinusoidal fore-and-aft asymmetry of amplitude A. The functional form was then

$$r(z) = (1 - z^2/4)^{\frac{1}{2}} + A \sin\left(\frac{\pi}{2} z\right) . \qquad (40)$$

A polar grid geometry was used with the same number N_y of nodes on the far-field boundary and body surface, and N_x nodes along each segment of the z-axis between the body and the far-field. A small offset could be added to the angles of the polar grid to make these asymmetrical about the r-axis. The spacing of the nodes could be varied on the z-axis and body surface, to change the grid density near the stagnation points relative to that near the body mid-point and the far-field.

3. RESULTS

3.1 Standard configuration

A "standard" configuration was chosen with far-field radius $R_0 = 10$ and $A = -0.3$ (equation (40)) which, with $N_x = 13$, $N_y = 21$ and conditions (35) and (38) satisfied, gave the nodal geometry shown in figure 3.

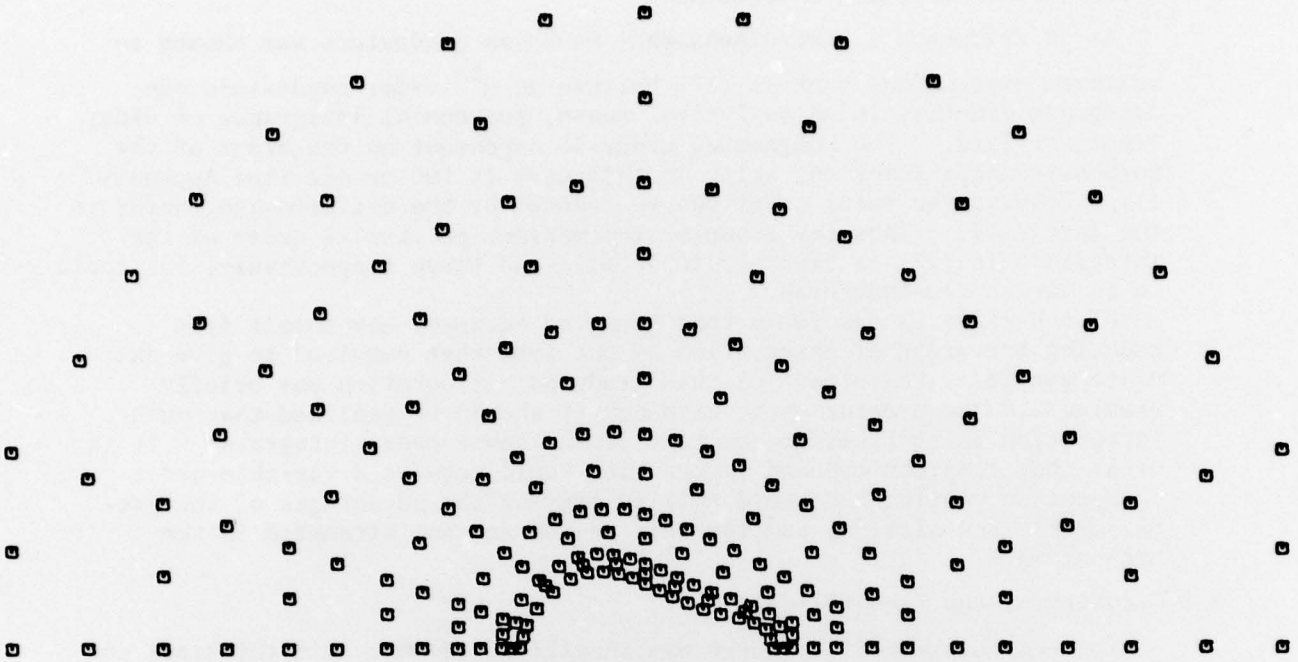

Figure 3. Nodal geometry for 13 x 21 grid

Initially $N_x = 17$ and $N_y = 21$ were chosen to take advantage of the local computer priority system (i.e. less than 2 min CPU time per calculation on an IBM 370), but it was subsequently found for some cases that N_x could be reduced to 13 without significantly changing the computed surface velocities. Single precision arithmetic was used, and at nodes where one of the field equations was omitted or replaced, the continuity equation was retained.

Accuracy of the results was judged by comparing surface velocities with those from an iterative method due to Albone(ref.3) in which the relative error is expected to be less than 1%. On figures 4 and 5 the present results are plotted with squares and triangles and those from the Albone program with the broken line, while the solid line represents the body profile.

3.2 Results from the (μ,v) formulation

The (μ,v) results shown on figure 4 were calculated using the standard configuration described above, with 'exact' integration and (29) and (32) applied except on the body surface. The axis elements shown in figure 3 also satisfy the additional condition

$$z_5 = z_7 = (z_1 + z_2)/2 \qquad (41)$$

in the notation of figure 2, which was found to significantly improve the results.

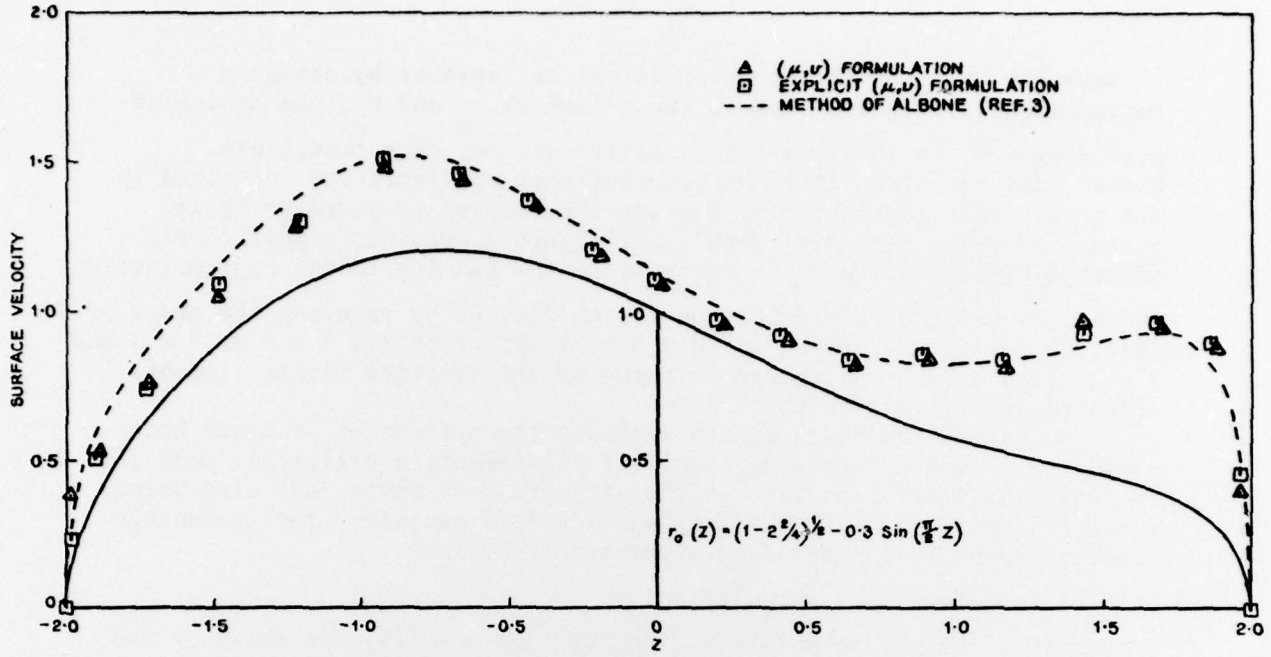

Figure 4. Results for surface velocity for optimum configurations

The (μ,v) results shown in figure 4 are generally close to the Albone values, however as a solution they exhibit a number of undesirable properties. For one thing the axial values of v, shown for the upstream axis in figure 5, do not follow the required monotonic decrease from 1 at infinity to zero at the stagnation point; the Albone program does not calculate off-body values and so these cannot be shown for comparison.

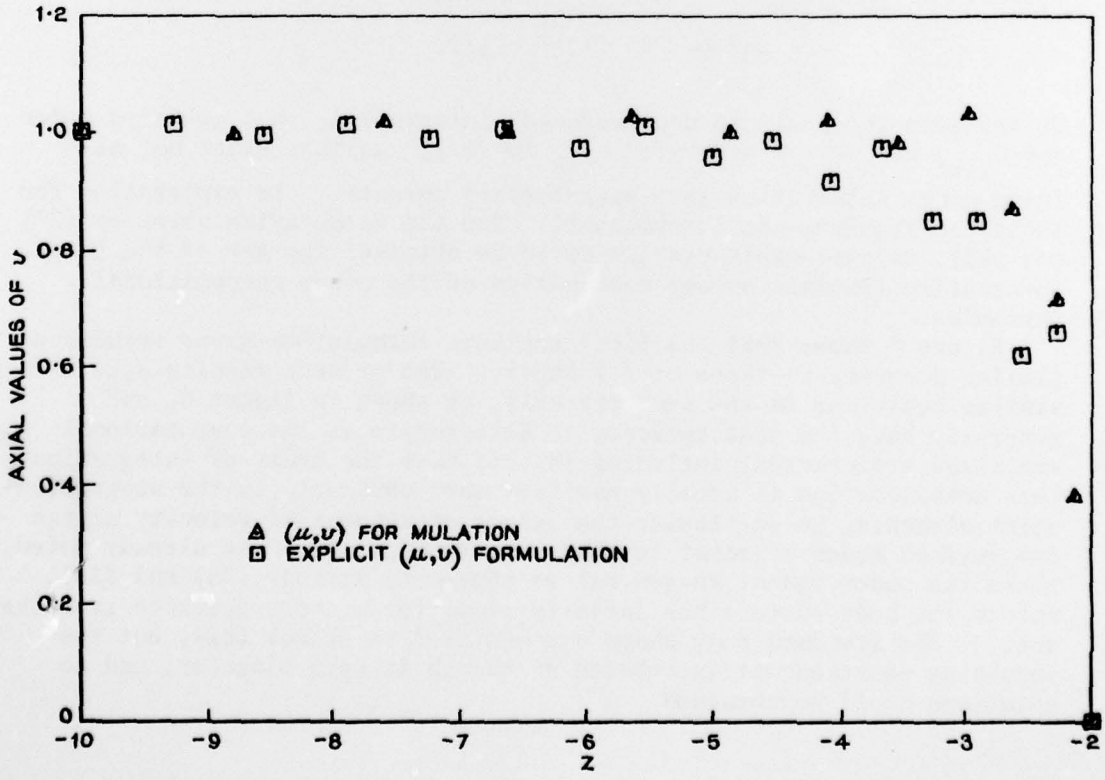

Figure 5. Values of longitudinal velocity on upstream axis

Secondly, the results shown could not be improved by changing computational variables such as the values of N_x and N_y, the choice of grid geometry, or the application of the various axis conditions. Rather, any variation from the computational configuration described in 3.1 above could significantly degrade the results compared to those given. However the (μ,v) results of figure 4 were not significantly affected by increasing R_0 to 20 provided the axial grid was appropriately scaled, by using double-precision arithmetic, or by reducing the order of integration (from orders 4 x 4 and 3 x 3) either to all 3 x 3 or 3 x 3 and 2 x 2, even though the change in value of the equation matrix elements affected was typically 30%.

Other variations investigated included the effects of grid and body asymmetry. The accuracy of results for a symmetric elliptical body (A = 0 in (40)) was similar to that of the standard body shape, all else being equal. However a small grid asymmetry seemed necessary for reasonable results, even for the standard asymmetrical profile.

3.3 Results from the (u,v) formulations

Results from the formulation given by (20) and (21) are shown by the triangles on figure 4. In this case the standard configuration was used with the original values $N_x = 17$ and $N_y = 21$, and it was found that the same regularised grid as used for the (μ,v) results was necessary to avoid poor results near the axis of symmetry, with the exceptions that (41) was not required but the body surface nodes in the axis elements needed to satisfy

$$z_6 = (z_2 + z_3)/2$$
$$\text{and } r_6 = (r_2 + r_3)/2. \qquad (42)$$

It was also necessary to use 'reduced' integration, that is third order for D_{jikl} and second order for C_{jik} in (17); neither exact nor all-third-order integration gave satisfactory results. No explanation for these two requirements is apparent. For the formulation given by (23) and (21), no reasonable results could be obtained for any of the three integration routines or any combination of the other computational variables.

Figure 4 shows that the first explicit formulation gives results of similar accuracy to those of 3.2 above. The present results also exhibit similar behaviour on the symmetry axis, as shown in figure 5, and generally have the same tendency to deteriorate as the computational variables are changed, including in this case the order of integration. This deterioration is usually manifest most obviously in the stagnation-point elements, in particular the values of tangential velocity at the two surface nodes adjacent to the stagnation points. As already noted, these two nodes cannot in general be chosen to satisfy (35) and (38), unless the body surface has infinite slope for a short distance from the axis. The standard body shape was modified to effect this, but the resulting equation matrix behaved as though it were singular, and no solutions could be obtained.

4. DISCUSSION

The results described above indicate that neither of the finite element formulations is at present a useful solution technique for the problem under consideration. However Galerkin formulations have been applied to similar problems in two dimensions, for example references 1 and 6. Certain aspects of the results already discussed indicate that the formulation of the problem near the axis of symmetry may contribute to the unsatisfactory nature of the solutions; for example, the behaviour of the v component along the axis as shown in figure 5, and the constraints imposed on the nodal geometry and nodal unknowns by application of the μ-component boundary condition, which are apparently also required in the (u,v) formulation.

Multiplying equation (1) by r to obtain a tractable finite element formulation, gives an equation that is trivially satisfied on the symmetry axis; this is also true of (2) in the (μ,v) formulation. Thus it might be expected that the Galerkin equivalent of (1) contributes little at an axial node since the weighting function (i.e. the shape function for the particular node) biases its effect towards the axial node. However in the (u,v) formulation where (2) has a non-trivial contribution on the axis, it was found that the single equation applied at the axial nodes had to be (1) to give the results in figure 4.

In addition to the behaviour near r = 0, a major difference between the present formulation and those of references 1 and 6 is that the latter use Green's theorem to include the boundary conditions implicitly in the field equations, as a boundary integral in the Galerkin formulation, while in the present case the boundary conditions appear only explicitly in the equation matrix. Of relevance here may be Fletcher's comments in reference 5 with respect to reduced integration, that results may be improved by relaxing the constraints on the polynomial form that the solution must assume in each element. Inclusion of the boundary conditions in a Galerkin sense, as in references 1 and 6, may ensure satisfactory behaviour without the constraints imposed by conditions such as (29), (32), (35) and (38). As already noted, the 'reduced' integration used here has little apparent effect on the (μ,v) results, but is required with the first (u,v) formulation if any reasonable results are to be obtained. Whether a changed integration scheme such as complete reduced integration could improve the results from the second (u,v) formulation, has not been determined.

No attempt has been made to change the type or order of finite element used from rectangular Serendipity. It was felt unlikely that the choice of element could be responsible for the apparent incompatibility in the formulations used.

5. CONCLUSIONS

A Galerkin finite-element method, using quadratic, rectangular, Serendipity elements, has been applied to the equations governing axisymmetric, inviscid incompressible flow. Three different formulations, using the same representation for longitudinal velocity and two different representations for the radial velocity component, have been tried.

The best results obtained have, surprisingly, shown only poor agreement with correct values and exhibit a number of undesirable properties, such as their dependence on an appropriate choice of grid geometry. None of the formulations has provided a useful aerodynamic calculation method.

NOTATION

A	amplitude of profile asymmetry (equation (40))
C_{ijk}, D_{ijkl}	coefficients from integration in iso-parametric plane (equation (17))
M_i	shape function in (r,z) plane for i^{th} node
N_i	shape function in (ξ,η) plane for i^{th} node
N_x	number of nodes on each segment of z-axis
N_y	number of nodes on far-field boundary and body surface
R	distance from origin in (r,z) plane, = $(r^2+z^2)^{\frac{1}{2}}$
R_0	radius of far-field
R_1, R_2	equation residuals in Galerkin formulation
S	region of (r,z) plane occupied by flow field
U	free-stream velocity
a_{ij}, b_{ij}, c_{ij}, d_{ij}	coefficients in matrix form of field equations (equations (13),(14),(20),(21),(23))
a_{ijk}	matrix coefficient (equation (23))
r,z	radial and longitudinal coordinates (figure 1)
r_0	functional form of body surface profile (figure 1)
u,v	radial and longitudinal velocity components (figure 1)
ξ,η	transformed coordinates in iso-parametric plane (figure 1)
μ	derived flow variable, = ru

Subscripts

i	referring to i^{th} node
1,2 etc.	referring to nodes 1,2 etc. (figure 2)
s	values on one side of element boundary
m	values on median line of element

REFERENCES

No.	Author	Title
1	Fletcher, C.A.J.	"The Application of the Finite Element Method to Two-Dimensional Inviscid Flow" WRE-TN-1606(WR&D), May 1976
2	Fletcher, C.A.J.	"Subsonic, Inviscid Flow by the Finite Element Method" WRE-TR-1858(W), August 1977
3	Albone, C.M.	"Fortran Programmes for Axisymmetric Potential Flow Around Closed and Semi-Infinite Bodies" Aero. Res. Council, C.P. No. 1216, 1972
4	Hess, J.L., and Smith, A.M.O.	"Calculation of Potential Flow About Arbitrary Bodies" Prog. Aero. Sciences, Vol.8, 1967
5	Fletcher, C.A.J.	"Improved Integration Techniques for Fluid Flow Finite Element Formulations" WRE-TR-1810(W), April 1977
6	Baker, A.J., and Manhardt, P.D.	"Finite Element Analysis of Low Speed Viscous and Inviscid Aerodynamic Flows" NASA Contractor Report CR-2908, October 1977

APPENDIX I

ELEMENT SHAPE FUNCTIONS

The shape function corresponding to a particular node is required to have the value one at that particular node and zero at all other nodes. The 'Serendipity' type form one family of the many functions which can be defined explicitly on the iso-parametric element (see figure 2) to have these properties.

For the quadratic rectangular elements used in this report, the shape functions of this family are defined as follows, where $\xi_i = \pm 1$ and $\eta_i = \pm 1$: at the corner nodes (ξ_i, η_i),

$$N_i(\xi,\eta) = \tfrac{1}{4}(1 + \xi\xi_i)(1 + \eta\eta_i)(\xi\xi_i + \eta\eta_i - 1); \tag{I.1}$$

at the side nodes (o, η_i),

$$N_i(\xi,\eta) = \tfrac{1}{2}(1 - \xi^2)(1 + \eta\eta_i); \tag{I.2}$$

at the side nodes (ξ_i, o),

$$N_i(\xi,\eta) = \tfrac{1}{2}(1 + \xi\xi_i)(1 - \eta^2). \tag{I.3}$$

Note that N_i may be either quadratic or linear in the coordinates (ξ,η).

In the (r,z) plane the function $M_i(r,z)$ corresponding to $N_i(\xi,\eta)$, and defined implicitly by equations (4) and (5) in Section 2.2 of this report, will have a different functional form in each element common to the i^{th} node, and by definition will be zero outside those elements.

DISTRIBUTION

	Copy No.
EXTERNAL	
In United Kingdom	
Defence Scientific and Technical Representative, London	1
R.A.E., Aero Department	2 - 3
Space Department	4
Weapons Department	5 - 6
Bedford	7
Library	8
R.A.R.D.E.	9
T.T.C.P., UK National Leader Panel W-2	10 - 13
Aeronautical Research Council	14 - 15
Aircraft Research Association (Bedford)	16
C.A.A.R.C. Secretary	17
National Lending Library of Science and Technology	18
Royal Aeronautical Society, Library	19
Professor O.C. Zienkiewicz, Department of Civil Engineering, University College of Swansea	20
Professor J.R. Whiteman, Department of Mathematics, Brunel University	21
In United States of America	
Counsellor, Defence Science, Washington	22
Defence Research and Development Attache, Washington	23
Applied Physics Laboratory, Johns Hopkins University	24
Air Force Armament Testing Laboratory	25
Ballistics Research Laboratories	26
Edgewood Arsenal	27
Eglin Air Force Base	28
N.A.S.A.	29 - 32
Naval Surface Weapons Center	
Dahlgren	33
White Oak	34
Naval Weapons Center	35
Naval Ship Research and Development Center	36
Picatinny Arsenal	37
Redstone Arsenal	38
T.T.C.P. US National Leader Panel W-2	39 - 42
Wright-Patterson Air Force Base, Library	43
American Institute of Aeronautics and Astronautics, Library	44

	Copy No.
Pacific Technical Information Services, Northrop Institute of Technology	45
Applied Mechanics Reviews	46
Arnold Engineering Development Center	47
A.R.O. Inc.	48
Sandia Corporation, Library	49
In Canada	
Defence Research Establishment, Valcartier	50
N.A.E., Ottawa	51
T.T.C.P., Canadian National Leader Panel W-2	52 - 55
University of Toronto, Institute of Aerospace Studies	56
Professor D.H. Norrie, Department of Mechanical Engineering, University of Calgary	57
In Europe	
A.G.A.R.D., Brussels	58 - 63
In India	
Aeronautical Development Establishment, Bangalore	64
Indian Institute of Science, Bangalore (Dept. of Aero. Engineering)	65
Indian Institute of Technology, Madras (Dept. of Aero. Engineering)	66
Hindustan Aeronautics Ltd., Bangalore	67
National Aeronautical Lab., Bangalore	68 - 69
Space Science and Technology Centre, Trivandrum	70
In Australia	
Chief Defence Scientist	71
Superintendent, Science and Technology Programmes	72
Director, Joint Intelligence Organisation (DDSTI)	73
Air Force Scientific Adviser	74 - 75
Army Scientific Adviser	76 - 77
Navy Scientific Adviser	78 - 79
Controller, Policy and Programme Planning	80
Deputy Chief Defence Scientist	81
Central Studies Establishment	82
Defence Information Services Branch (for microfilming)	83
BDRSS, Canberra	84

	Copy No.
Defence Information Services Branch for:	
United Kingdom, Ministry of Defence, Defence Research Information Centre (DRIC)	85
United States, Department of Defense, Defense Documentation Center	86 - 97
Canada, Department of National Defence, Defence Science Information Service	98
New Zealand, Department of Defence	99
Australian National Library	100
Chief Superintendent, Aeronautical Research Laboratories	101
Superintendent, Aerodynamics Division, ARL	102
D.A. Secomb, for data exchange agreement, ARL	103
Superintendent, Mechanical Engineering Division, ARL	104
Library, Aeronautical Research Laboratories	105
Library, Materials Research Laboratories	106
Defence Library, Campbell Park	107
Aircraft Research and Development Unit, Edinburgh	108
G.A.F., Department of Productivity, Melbourne	109
RAAF Academy, Point Cook	110
C.A.C.	111
Institute of Engineers, Australia	112
Dr C.A.J. Fletcher, Department of Mechanical Engineering, University of Sydney	113
WITHIN DRCS	
Chief Superintendent, Weapons Systems Research Laboratory	114
Superintendent, Aeroballistics Division	115
Head, Ballistics Composite	116
Principal Officer, Dynamics Group	117
Principal Officer, Aerodynamics Research Group	118
Principal Officer, Ballistics Studies Group	119
Principal Officer, Field Experiments Group	120
Principal Officer, Flight Research Group	121
Author	122
DRCS Library	123 - 124
AD Library	125 - 126
Spares	127 - 150